29 August 2025
fred.laats@cern.ch

Crosstalk characterisation of the readout electrodes for the ALLEGRO ECAL

Fred Eerik Laats
CERN, CH-1211 Geneva, Switzerland

Summary

This report presents an initial study of signal cross-talk in a prototype readout electrode developed for a noble liquid electromagnetic calorimeter of the Future Circular Collider (FCC). Different signal tracing and shielding configurations were tested using direct signal readout and readout with a fanout board. The influence of the readout setup on signal amplitude and oscillations was also evaluated. Results show that x-talk is highest in neighbouring cells, with logical tracing exhibiting strong localised x-talk and optimised tracing showing a more even distribution. Towers with wider vertical shielding, particularly tower 13, demonstrated the lowest x-talk, confirming the effectiveness of this approach while highlighting the trade-off with capacitance and noise. These measurements provide a useful basis for future detector design studies.

Contents

1 Introduction

The Large Hadron Collider (LHC) is one of the largest scientific projects in the world, resulting from years of international collaboration and remarkable achievements in physics and engineering. With the discovery of the Higgs boson, the Standard Model (SM) was completed, but many questions remain unanswered. Scientists now aim to discover new phenomena, which may appear at collision energies beyond what the LHC can currently reach.

While the LHC has been a major step forward in particle physics, plans for a Future Circular Collider (FCC) represent the next stage in exploring the fundamental structure of our universe. The proposed 80–100 km ring, to be built alongside CERN's existing infrastructure, would enable deeper studies of the Higgs boson and provide a more precise understanding of the SM. More importantly, the FCC is designed to address the shortcomings of the SM and open the door to research beyond it (BSM physics). This includes questions about the matter–antimatter imbalance, the origin of neutrino masses, and the nature of dark matter. [1]

The 27 km collider ring was commissioned in 1989, with the Large Electron-Positron (LEP) collider as its first operation mode. In 2008, the LHC operation mode began, using the same tunnel previously employed for LEP. The LHC currently hosts four major experiments: ATLAS, CMS, LHCb, and ALICE. These detectors are placed in the straight sections of the collider and allow researchers to reconstruct particle paths after collisions, as well as to collect data on particle energies and momenta.

One of these detectors, ATLAS, is a general-purpose experiment designed to observe a wide range of phenomena. It is made up of six different detecting subsystems, arranged concentrically, to capture as much information as possible from each collision. The detector itself is cylindrical, measuring 46 m in length and 25 m in diameter, and is located in a cavern 100 m underground. The internal structure of the detector is shown in Figure 1.

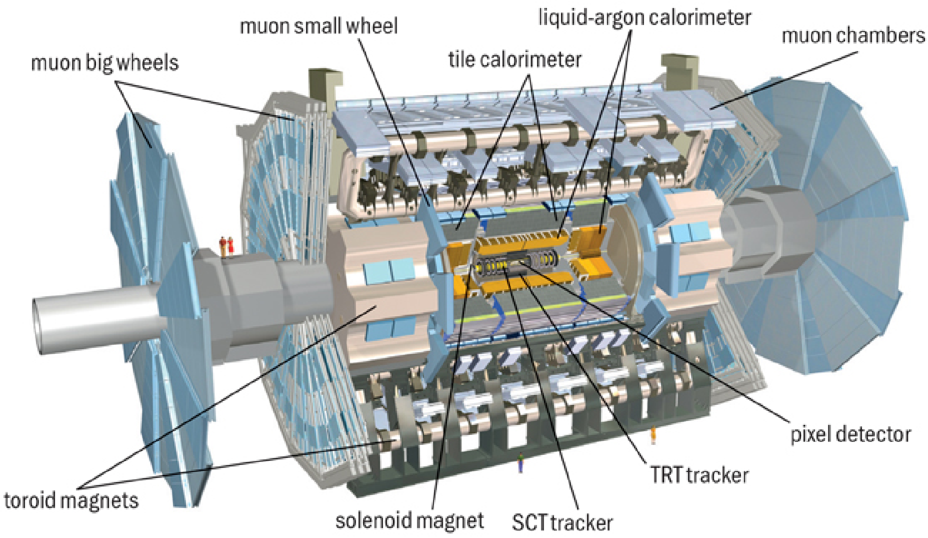

Figure 1: ATLAS detector. [3]

The ATLAS experiment features a liquid-argon calorimeter with accordion-shaped electrodes, designed to provide full azimuthal coverage so that no electron or photon would go undetected. While this approach successfully achieved full coverage, the mechanical production of the accordion layers with spacers was highly complex and introduced limitations on both accuracy and size.

Recent technological advancements now make it possible to replace the accordion-shaped design with flat printed circuit boards (PCBs), offering higher granularity and simpler manufacturing and construction. This concept is planned to be applied in the proposed ALLEGRO detector for the FCC.

1.1 ALLEGRO

ALLEGRO, which stands for *A Lepton-Lepton collider Experiment with Granular Read-Out*, is a proposed detector concept for the first stage of the FCC, the future circular electron–positron collider (FCC-ee) at CERN. It will employ a highly granular noble-liquid sampling electromagnetic calorimeter, with a strong focus on particle-flow reconstruction and particle identification performance.

Noble-liquid calorimetry is a well-established technology, successfully implemented in several high-energy physics experiments, including DØ at the Tevatron, ATLAS at the LHC, and NA62 at the SPS. In addition to their extreme radiation hardness, noble-liquid calorimeters are known for their excellent energy resolution, linearity, stability, uniformity, and timing performance, all at a reasonable cost. Recent advances in PCB technology and customised solutions now make it possible to add high granularity on top of these advantages. These combined properties make the technology a strong candidate not only for FCC-ee but also for future FCC-hh experiments, underlining the broader importance of this detector concept. [4]

The detector will consist of alternating layers of absorbers, readout electrodes, and liquefied noble gas as the active material, which together enable the reconstruction of electrons and photons passing through. The geometry of the detector is shown in Figure 2, where the readout electrodes are inclined at an angle of 50°. This inclination allows particles to traverse several electrodes and absorbers, thus optimising data collection. It also makes sure that the particle is not able to escape the detector without interacting with any absorber at all.

The PCBs will be arranged in a barrel configuration and will consist of a total of 1536 layers. The signal will be read out at the end of each plate, preventing any interference with the particles passing through the detector. The absorber layers, typically made of lead or tungsten, convert incoming particles into a shower of lower-energy secondary particles. These, in turn, ionise the noble liquid between the layers, producing an electric current that can be measured. By combining all detected currents, physicists can reconstruct the energy of the original particle entering the detector. Each of these readout electrodes has a segmented configuration, meaning the electromagnetic shower can be reconstructed very precisely.

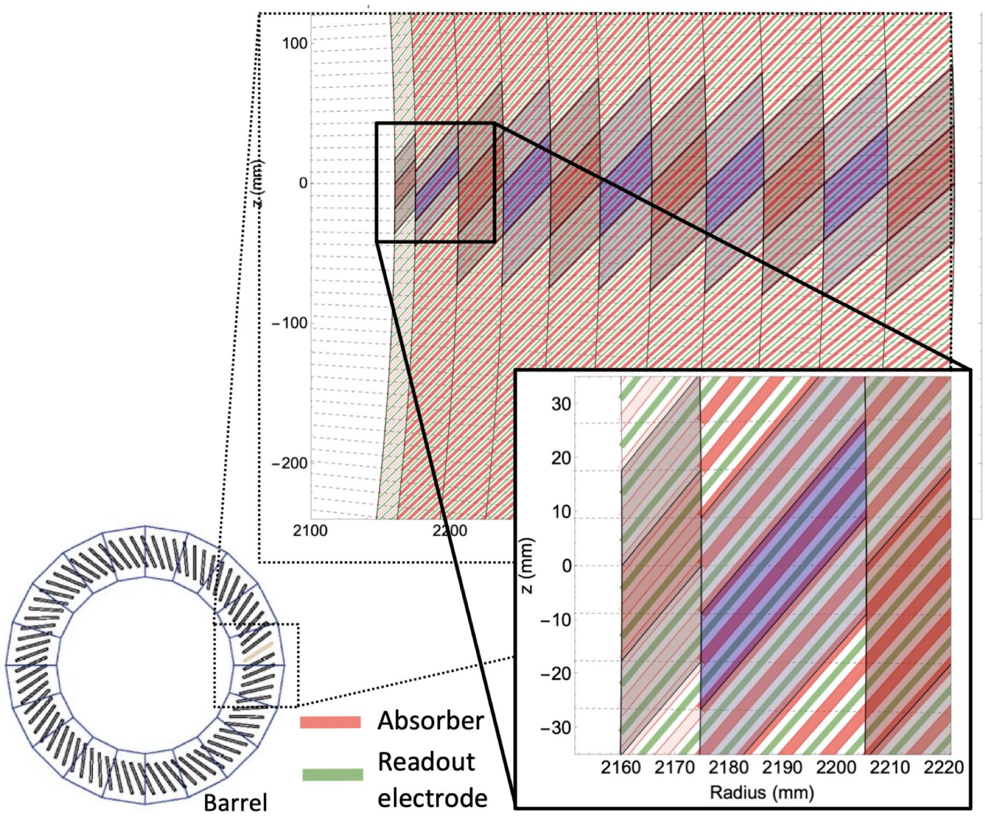

Figure 2: ECAL barrel baseline geometry with 11 longitudinal layers. [2]

This project focuses mainly on minimising the cross-talk of signals between the different cells of the high-granularity detector. The PCBs used contain multiple signal traces placed next to each other, which can lead to signal leakage between the main signal line and adjacent lines. This can degrade the signal quality and the energy resolution. This study aims to determine the optimal signal line structure, together with a shielding configuration, in order to minimise cross-talk (x-talk) and achieve the best possible signal quality.

A dedicated test setup with different tower configurations was used to measure x-talk and to compare simulated signals with experimental results.

2 Experimental Setup

2.1 Printed Circuit Board

A 7-layer printed circuit board (PCB) with 16 towers was produced to test the effectiveness of different signal tracing and shielding configurations. Each tower consists of 13 to 17 cells, with the signals mainly read out from pins located at the end of the tower. At the beginning of each tower, slimmer strips are included to improve particle separation. These strips are placed in one of the first layers of a tower, helping to distinguish particles that travel close to each other. The PCB layout is shown in Figure 3.

Figure 3: Prototype PCB for testing the different tower configurations used in the readout electrode.

The internal structure of the PCB is shown in Figure 4. The 7-layer configuration begins with the high-voltage top and bottom layers, whose purpose in the detector is to direct electrons towards the signal pick-up. Beneath these lies the signal pickup layer, which collects the signal generated when charges drift in the noble liquid. Under this layer are ground shields, placed above and below the signal extraction line, designed to minimise x-talk with neighbouring lines and cells. Finally, the signal extraction layer guides the signal to the readout.

The shielding configuration described here represents the baseline for the towers. The detailed configurations for each tower are provided in Appendix A. Since the signal lines run in close proximity, shielding helps to reduce the induced signal in parallel lines. However, adding additional shielding also increases capacitance, which leads to higher noise levels. These two effects must therefore be carefully balanced to maximise performance.

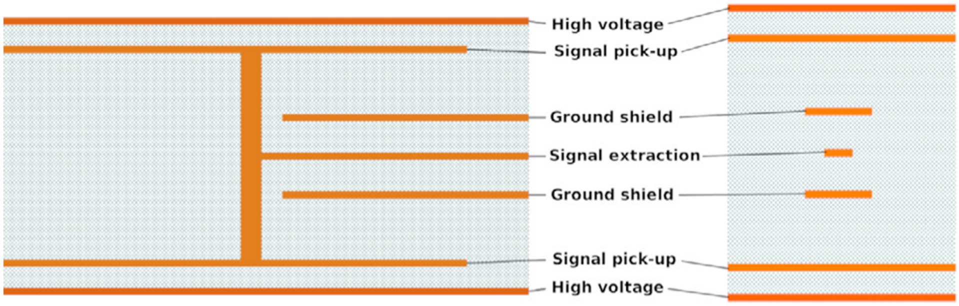

Figure 4: Cross-sectional views of the layers of the readout electrode prototype. Copper is shown in orange and dielectric in gray. The left-hand-side figure shows a side view of a cell from an angle perpendicular to the signal propagation direction. The right-hand-side figure shows the structure along the signal propagation direction.

A cutout of the beginning of the PCB internal structure is shown in Figure 5. Various signal tracing and shielding configurations are implemented here, with the goal of testing different layouts to achieve the lowest possible x-talk. The signal traces are shown in pink.

Injection vias are placed on top of the pads, allowing direct signal deposition into the cells. In addition, cells 8 and 5 include injection pairs, which provide both signal injection and a ground connection. A summary of all tower-specific configurations is given in Table 1.

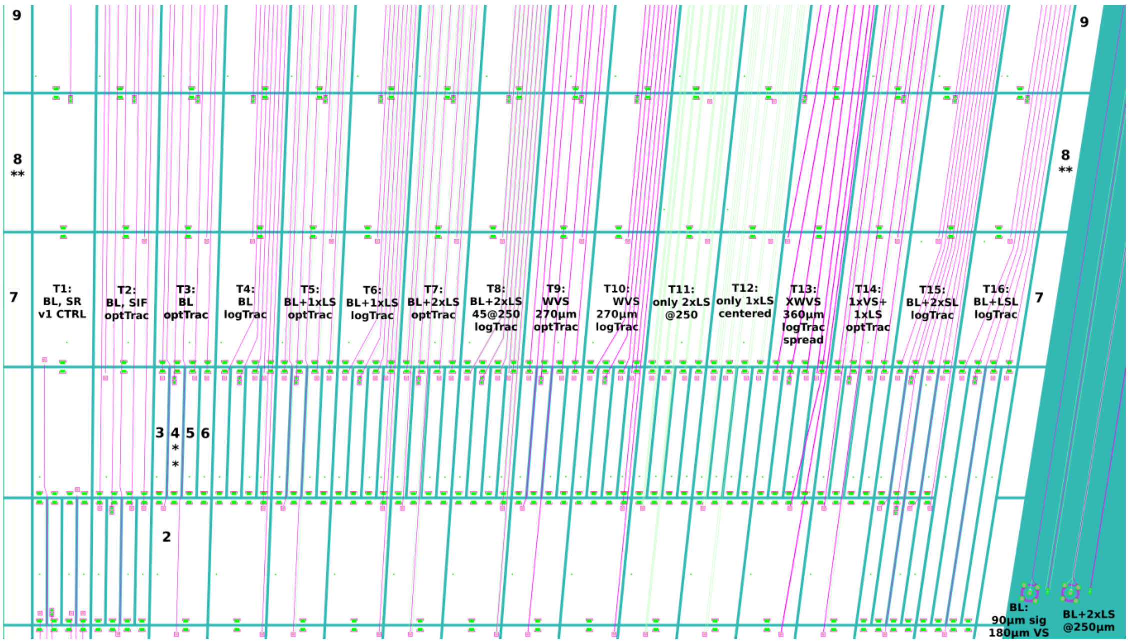

Figure 5: The tower configuration drawing of PCBv2.

Table 1: Tower configurations

Tower	Trace configuration	Shielding configuration
T1	optTrac	BL, SR v1 CTRL
T2	optTrac	BL, SIF
T3	optTrac	BL
T4	logTrac	BL
T5	optTrac	BL+1xLS
T6	logTrac	BL+1xLS
T7	optTrac	BL+2xLS
T8	logTrac	BL+2xLS 45@250
T9	optTrac	WVS 270 µm
T10	logTrac	WVS 270 µm
T11	optTrac	only 2xLS @250
T12	optTrac	only 1xLS centered
T13	logTrac spread	XWVS 360 µm
T14	optTrac	1xVS + 1xLS
T15	logTrac	BL+2xLS
T16	logTrac	BL+LSL

Abbreviations: BL = baseline configuration; LS = lateral shield; LSL = long strip layer; VS = vertical shield; WVS = wide vertical shield; XWVS = extra-wide vertical shield; SIF = strips in front; SR = split readout;

Two different configurations of signal traces were implemented: optimal tracing (optTrac) and logical tracing (logTrac). In the logTrac configuration, the signal lines for the cells run in a logical order from 1 to 14. This means that the trace of cell 1 is placed at the edge of the tower, followed by cell 2, and so on. In the optTrac configuration, the ordering is optimised, as shown in Figure 6, to minimise the distance over which two signals run in parallel. This may reduce x-talk, since a shorter parallel overlap is expected to result in a smaller influence between neighbouring lines.

Tower 1 differs from the others by having a split readout section, where cells 1-7 are read out from pins on the opposite side of the board. Tower T13 features a spread logTrac configuration, in which the signal traces are routed with wider spacing across the tower width. Instead of the compact, parallel arrangement of standard logTrac, the spread layout distributes the traces further apart, providing a geometry to test whether increased lateral separation reduces x-talk between adjacent channels.

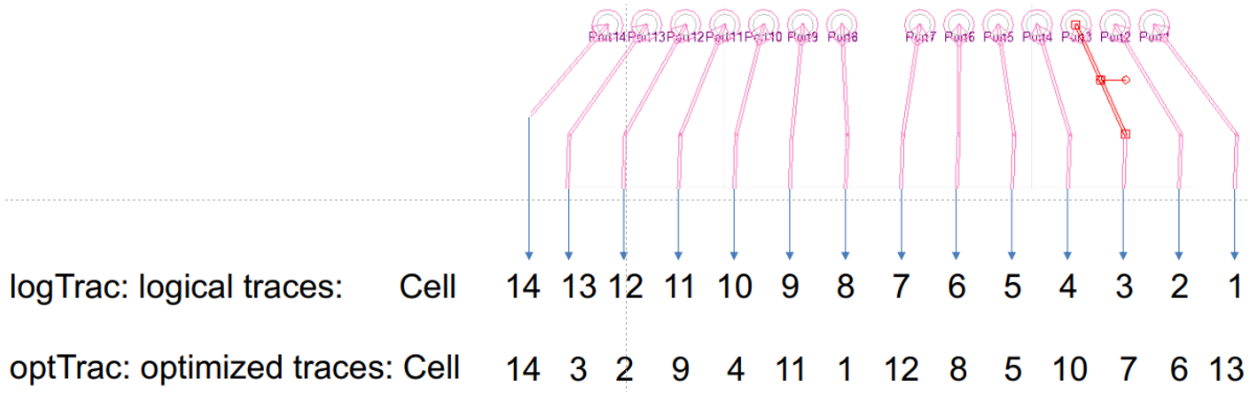

Figure 6: Signal traces

An image of the setup used can be seen in Figure 7. A signal generator is used to inject a shark-fin shaped signal. The decay time of the signal is 300 ns, the cycle length is 5 ms, and the amplitude is 1 V. This signal is chosen because it mimics what happens in reality: when a particle ionises the noble liquid, the charge is collected on the signal lines. At the start the intensity is highest, but as the ions get collected the signal falls off, which creates the shark-fin shape.

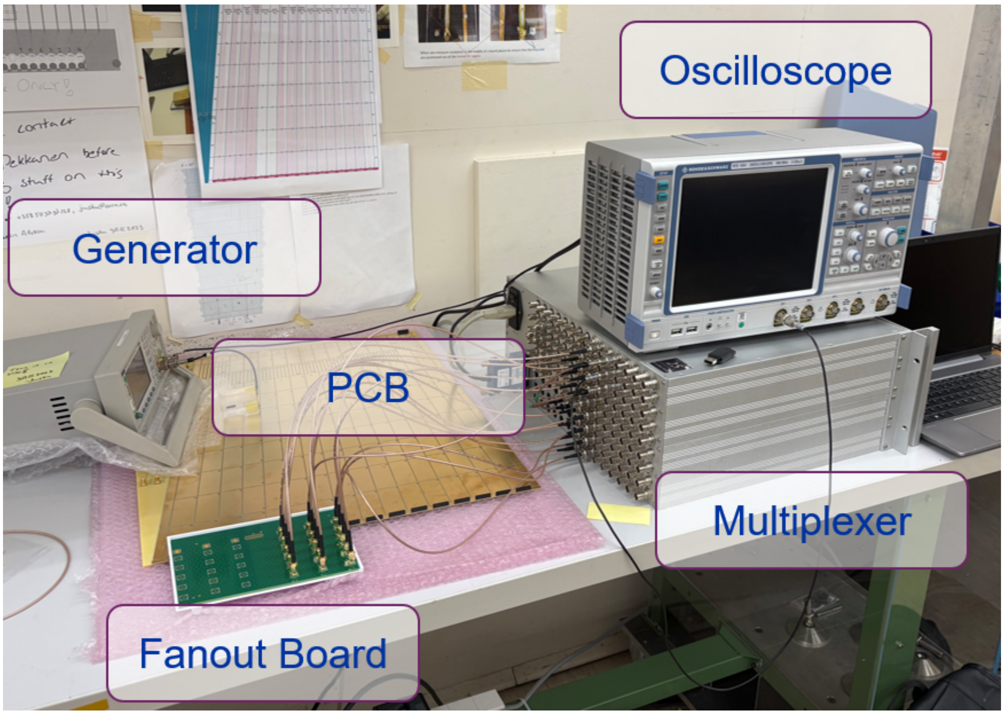

Figure 7: Experimental setup including the signal generator, PCB, fanout board, multiplexer, and oscilloscope.

The signal can be injected directly to the PCB through injection vias, or through the fanout board. Injecting from the vias simulates the situation where the signal is generated inside a cell in the middle of the board, which aims to reproduce the physics more accurately.

Injecting through the fanout board makes the measurements easier, but loses a bit of accuracy compared to the situation described above. It is also important to keep in mind that every extra piece of equipment between the signal and the readout can slightly change the signal characteristics.

The signal can either be collected manually by attaching cables directly to the PCB, or through the fanout board. The fanout board is an extra PCB that can be connected to the signal pins, allowing the measurement of all x-talks simultaneously. When using the fanout board, the signal is routed through a multiplexer. Since the oscilloscope can only record two channels at the same time, the multiplexer cycles through the cells. Using a MATLAB script connected to a laptop, the multiplexer cycles through the channels. Finally, the signal is sent to the oscilloscope, where the data is saved. It is important to note that the main signal must be terminated by measuring it with the oscilloscope, otherwise additional x-talk is observed in the other cells.

2.2 Signal Processing and x-talk Definition

To analyse the signals from the PCB read-out, the raw waveforms are shaped with a CR–RC^2 filter. Shaping helps to clean up the signal by improving the signal-to-noise ratio, removing noise, and giving a clear pulse height for comparison. In this project three shaping times were tested: 20 ns, 50 ns, and 200 ns. A short shaping time like 20 ns reduces pile-up but makes the noise stand out more. A long shaping time like 200 ns smooths out the noise, but pile-up becomes more of an issue. The 50 ns shaping time sits in between as a compromise. Testing all three makes it possible to see how the cross talk behaves under different conditions and to find the best settings for the FCC-ee.

X-talk is defined as the ratio of the maximum value of the shaped signal observed in an another channel compared to the maximum value of the shaped signal in the injected channel. This provides a quantitative measure of unwanted signal leakage between cells in a tower.

For convenience, this ratio is often expressed as a percentage:

$$R_{\text{x-talk}}(\tau)\,[\%] = \frac{\max\left(V_{\text{x-talk, shaped}}(t;\,\tau)\right)}{\max\left(V_{\text{direct, shaped}}(t;\,\tau)\right)} \times 100. \tag{1}$$

A low x-talk ratio indicates effective shielding and trace optimisation in the PCB design, while a high ratio suggests strong coupling between measured cells. The dependence of $R_{\text{x-talk}}$ on shaping time τ provides insight into the frequency response of the detector and the effectiveness of different tower configurations.

An example of the measured signal is shown in Figure 8. The dashed line represents the raw signal, while the solid line shows the shaped signal. A shaping time of 50 ns was used. For better visibility on the plot, the x-talk signal and its shaped version are amplified by a factor of 100.

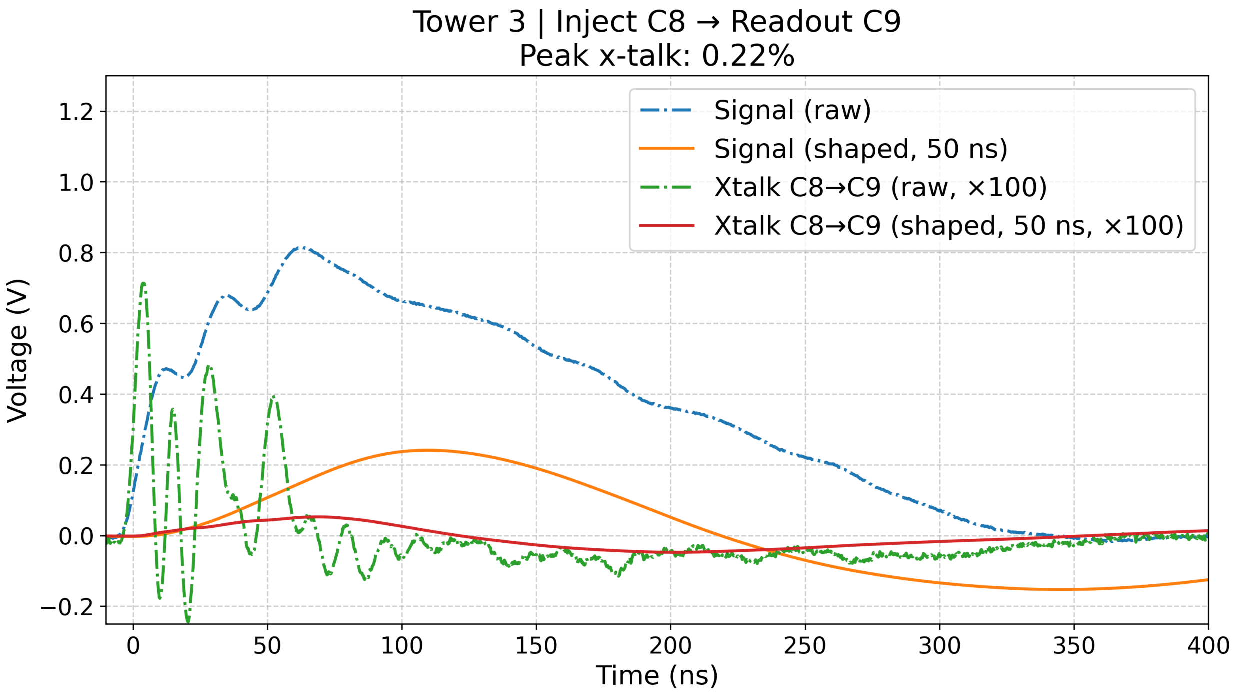

Figure 8: Example plot of the measured direct signal and the corresponding x-talk signal.

3 Results

3.1 Influence of setup configuration

First, the influence of the readout setup was investigated. Four configurations were tested:

1. pins connected directly to the oscilloscope,
2. pins connected to the oscilloscope through the multiplexer,
3. pins connected through the multiplexer using an additional *bridge* connection in the multiplexer,
4. readout through the fanout board, then through the multiplexer using the long *bridge* path.

The *bridge* in the multiplexer was tested because each multiplexer column provides 8 channels. To read all 14 cells, two columns must be used, which requires bridging between columns inside the multiplexer. This study checks how these routing choices affect the measured waveform and the apparent x-talk. For all measurements, a shaping of 50 ns is used.

In Figure 9, the main signal can be seen for the different configurations, when injecting from cell 8 of tower 10 using the injection pair. It is visible that an added complexity in the readout configuration reduces the amplitude of the signal. Compared to the base case of manual readout with no multiplexer, the fanout board readout with a long multiplexer connection reduces signal amplitude by 12%, which can definitely have an effect on the x-talk.

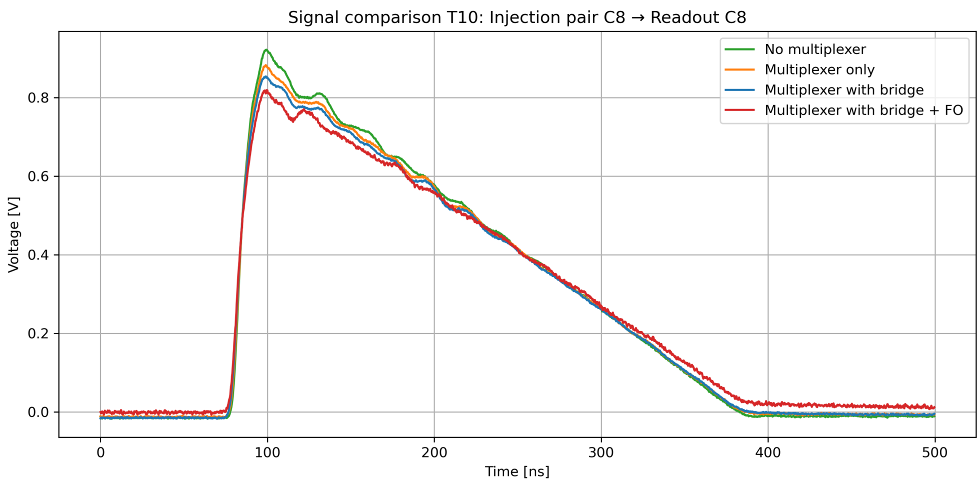

Figure 9: Signal recorded in C8 T10 with the oscilloscope in 4 different readout configurations, when injecting through the injection pair.

Figure 10 shows the x-talk signals for the four different readout configurations in neighbouring cells 7 and 9. Since T10 is a logical tracing tower, the x-talk is expected to be highest in these cells. It can be seen that the first three configurations have only a small effect on the signal, and after shaping, the calculated x-talk values remain very similar. In contrast, the fourth configuration with the fanout board introduces a clear change, with reduced signal amplitude and visible oscillation changes. To better understand this effect, additional tests were carried out using different fanout board configurations.

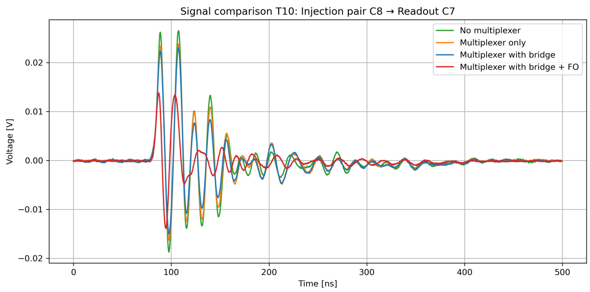

(a) Measured x-talk for readout cell C7.

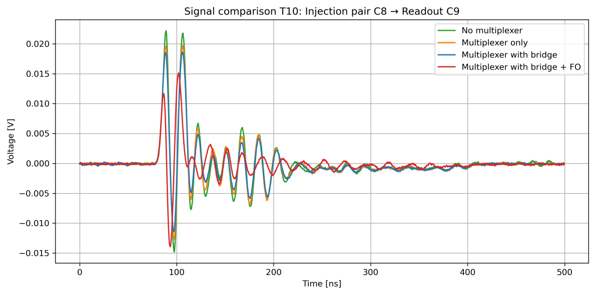

(b) Measured x-talk for readout cell C9.

Figure 10: Comparison of the measured x-talk for two neighbouring readout cells, when injecting in C8 injection pari in T10.

As can be seen in Figure 11, the significant change in the waveform only occurs when using the fanout board with a longer multiplexer configuration. As a result of this, further measurements avoided the use of multiplexer together with *bridge*, when measuring through the fanout board.

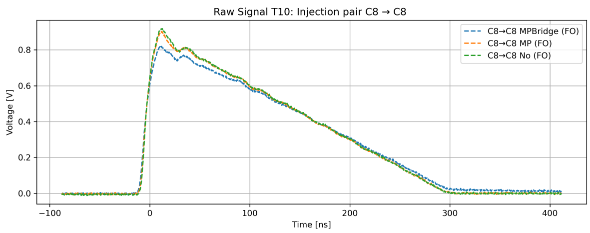

(a) Measured raw main signal for readout cell C8

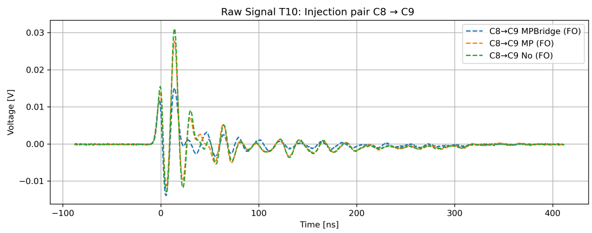

(b) Measured raw x-talk for readout cell C9.

Figure 11: Measured raw signals in T10 using different configurations involving the different fanout board configurations

Next, the reproducibility of the results was tested. Figure 12 shows the measured x-talk in T9. The measurements were done using the fanout board readout and no *bridge* in the multiplexer. The measurements were performed on different days and after reconfiguring the fanout board, in order to test whether the results remain stable under slightly different conditions. The comparison shows absolute differences in the range of 1–10% between the two datasets. This demonstrates that the results are generally reproducible and that the error between independent measurements can be considered small. Since the setup is highly sensitive to external factors such as nearby electronics and even fluctuations in the CERN electricity grid, a variation of this size can be regarded as acceptable. Overall, this confirms that the measurement procedure is robust and that the observed x-talk behaviour is not dominated by random instabilities in the setup.

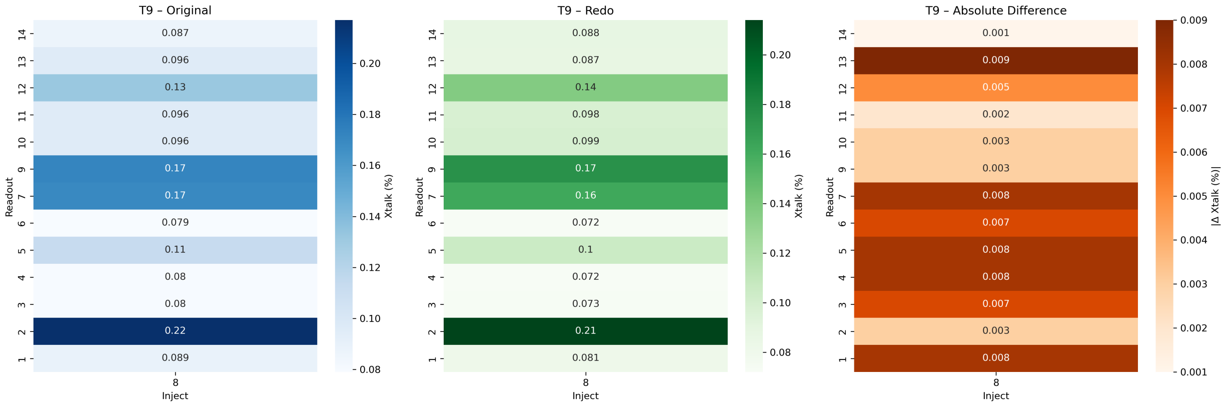

Figure 12: Reproducibility test for T9. The figure shows measured x-talk heatmaps taken on different days with different fanout board configurations, along with a heatmap of the absolute differences.

3.2 Heatmap Results of PCB Crosstalk

First, all towers were measured in order to create a heatmap covering the main towers of interest. For this study, towers 3, 4, 5, 6, 7, 8, 9, 10, and 13 were considered, as they show comparable x-talk levels but feature different shielding configurations. Figure 13 shows the results for injection into the C8 injection pair. The heatmap is arranged to resemble the physical layout of the board, making it easier to compare directly with the real PCB geometry. The towers are shown along the x-axis, while the y-axis corresponds to the readout cell number.

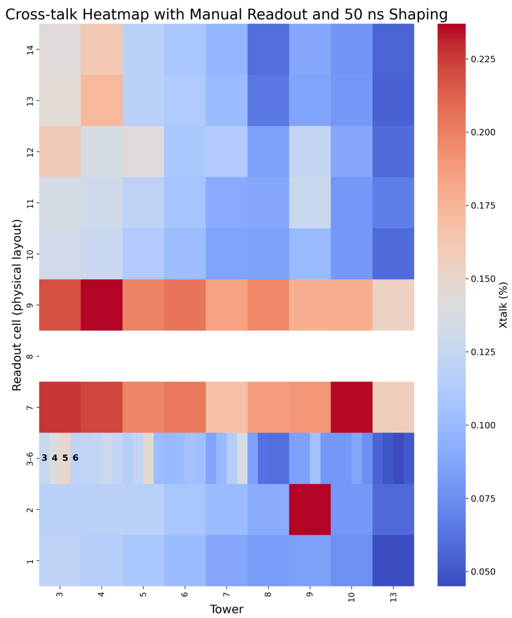

Figure 13: X-talk heatmap injection C8 with manual readout and 50 ns shaping. The x-axis shows the measured towers and the y-axis represents the physical layout of the readout cells.

It can be seen that the x-talk generally decreases for the higher tower numbers. This trend is mainly due to the fact that the higher towers include more shielding, which is designed to minimise x-talk. In all cases, the highest x-talk is observed in the cells directly adjacent to the injection line, for both optTrac and logTrac configurations. For the optTrac case, the neighbouring signal lines to injection line 8 are cells 5 and 12, and both show clear additional x-talk. Among the tested towers, T13 performs the best. Its configuration, with extra-wide vertical shield spread and logical tracing, demonstrates that increasing the vertical shield width is effective in reducing x-talk. However, it should be kept in mind that adding more copper shielding also increases capacitance and noise, meaning that an optimal balance between shielding and noise must be found. However, the manual readout method is very prone to imperfect pin connections and thus human error can cause issues with the measurement results. For example the higher cells of T4 increase in x-talk, however the opposite is expected. Additionally, it is important to note that T9 C2 has a misplaced shield, leading to a high x-talk in all subsequent plots.

To allow for more consistent measurements, the fanout board was implemented. This setup allows the collection of all x-talk signals through the multiplexer, ensuring more reliable pin contact and enabling straightforward measurement of all channels. However, the use of the fanout board slightly alters the signal, and it must be considered that some x-talk characteristics may be introduced or filtered out by the additional electronics. The results for injection from the C8 injection pair and readout using the fanout board are shown in Figure 14.

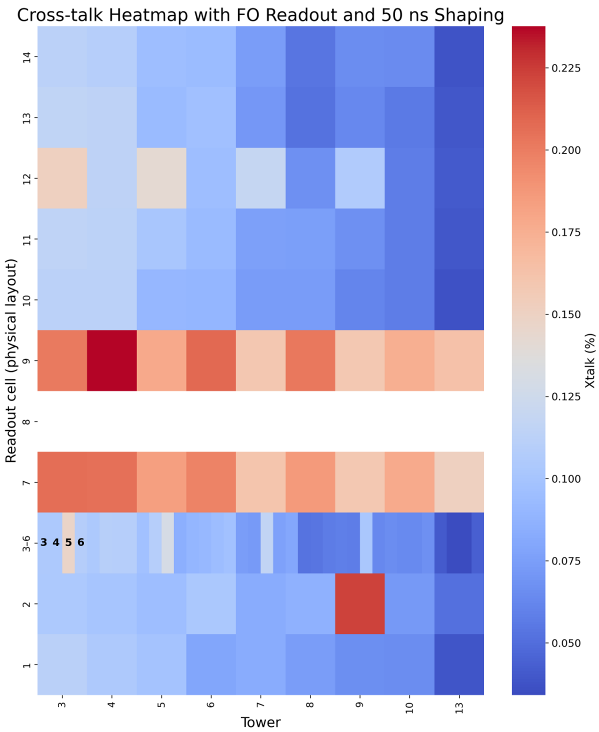

Figure 14: X-talk heatmap injection C8 with fanout board readout and 50 ns shaping. The x-axis shows the measured towers and the y-axis represents the physical layout of the readout cells.

In this configuration, the effect of the optTrac layout becomes very clear. For towers with optTrac, the cells with the highest x-talk are 12 and 5, which are the signal lines directly adjacent to the injection. In contrast, the logTrac towers follow a different trend, the further a cell is from the injection line, the lower the measured x-talk. Once again, T13 performs best in suppressing x-talk, with towers 7, 8, 9, and 10 also showing good performance. Overall, the optTrac configuration leads to x-talk that is more evenly distributed across cells, whereas in the logTrac case the x-talk is strongly concentrated in the neighbouring cells and drops off with distance. Even though the max x-talk is higher in logTrac towers, the average x-talk is lower than in the same shielding configuration optTrac cells.

Finally, there is also the option of injecting the signal through the fanout board. For comparison, this was again carried out using the C8 injection pair. It is important to note that for all x-talk measurements the main signal was terminated by collecting it in the oscilloscope. This termination has been shown to reduce unwanted oscillations in the x-talk measurements. However, this procedure cannot be applied when injecting from the fanout board, which may lead to higher x-talk values. This limitation should be kept in mind when interpreting the results. The corresponding measurements are shown in Figure 15.

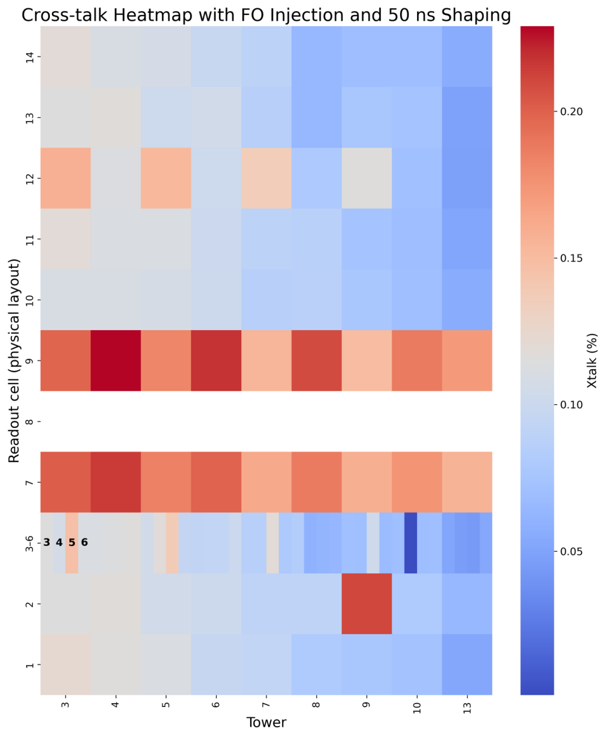

Figure 15: X-talk heatmap fanout board injection C8 with fanout board readout and 50 ns shaping. The x-axis shows the measured towers and the y-axis represents the physical layout of the readout cells.

It can be seen that the average x-talk values are noticeably higher than in the previous cases. As mentioned earlier, this is most likely caused by the inability to terminate the main signal when injecting through the fanout board. Nevertheless, the same general trends are observed: in the logTrac towers the x-talk decreases with distance from cell 8, while in the optTrac towers the adjacent signal lines also show higher x-talk. Once again, T13 performs best, confirming that its shielding configuration is effective in reducing x-talk.

Finally, one more heatmap was plotted, when injecting to one of the strip cells in the beginning, which also has an injection pair. The plot can be seen in Figure 16.

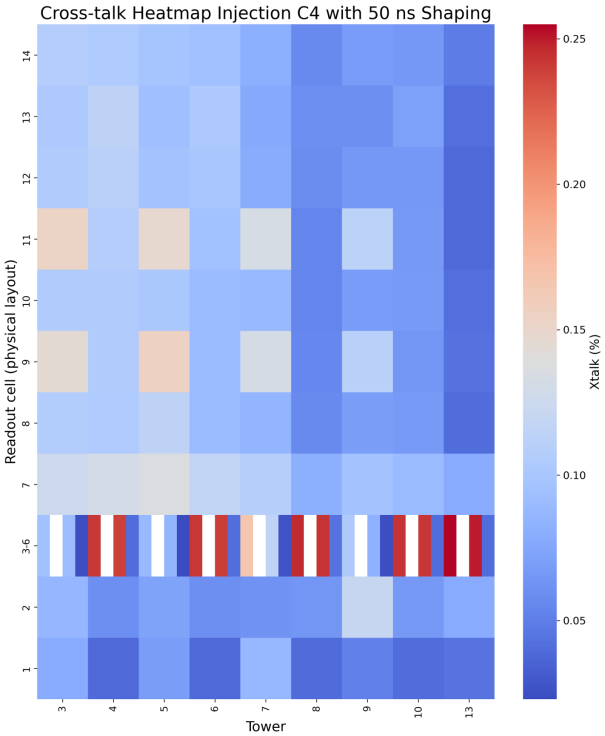

Figure 16: X-talk heatmap fanout board injection C8 with fanout board readout and 50 ns shaping. The x-axis shows the measured towers and the y-axis represents the physical layout of the readout cells.

When looking at the overall trends, it is same for when injecting through C8. The optimal tracing signal trace x-talk is clearly visible. While before the logical tracing would have lower x-talk averages, this time optimal tracing has lower averages. Mainly due to the very high neighbouring cell x-talk in the logical trace ordering. Additionally, T9 outperforms T13 in this case. Overall, this difference in performance is good to keep in mind, as when the signal generated in the strips behaves differently when compared to the situation where the signal is generated in the cell.

3.3 Conclusion and Outlook

These tests have provided valuable insight into how x-talk behaves under different shielding configurations, as well as the influence of the measurement setup. Among the towers tested, T13 showed the best performance, followed by T9 and T10. T13 uses an extra-wide vertical shielding configuration, while T9 and T10 use very-wide vertical shielding. This trend confirms that wider vertical shields are effective in reducing x-talk. However, as mentioned earlier, increasing the shield width also raises capacitance and electronic noise, so these effects must be carefully balanced when choosing a design for the detector. One possible reason why T13 performed best may be the influence of neighbouring towers: T12 and T14 have less shielding on their top and bottom sides, which could have reduced the overall x-talk measured in T13.

Further studies should be carried out with the high-voltage pads connected, as in this study they were left separated, while in the final detector design they will be active. In addition, absorbers are expected to influence the x-talk behaviour and should also be included in future tests. Overall, while no fully conclusive results can be drawn at this stage, this initial study provides an important first step towards understanding the interplay of shielding, tracing, and setup effects. It also serves as a foundation for future measurements with more realistic detector conditions.

References

[1] A. Abada, M. Abbrescia, S. S. AbdusSalam, and et al. Fcc physics opportunities. *European Physical Journal C*, 79(6):474, 2019.

[2] ALLEGRO Collaboration. Allegro ecal barrel plots, 2025. Accessed: 2025-08-27.

[3] ATLAS Collaboration. The atlas calorimeter, 2025. Accessed: 2025-08-27.

[4] Juska Pekkanen. Allegro fcc-ee detector concept noble liquid calorimetry. *Nuclear Instruments and Methods in Physics Research Section A: Accelerators, Spectrometers, Detectors and Associated Equipment*, 1069:169921, 2024.

Appendices

A Tower shielding configurations

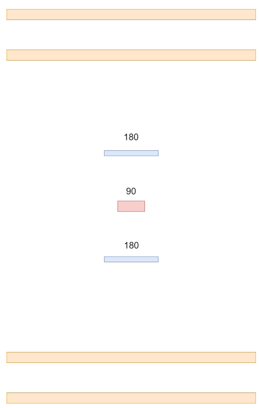

Figure 17: Shielding configuration for Towers 1, 2, 3, 4, 15, 16. Signal line shown in red and shields in blue.

Figure 18: Shielding configuration for Towers 5, 6. Signal line shown in red and shields in blue.

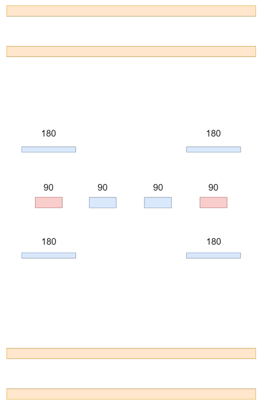

Figure 19: Shielding configuration for Towers 7, 8. Signal line shown in red and shields in blue.

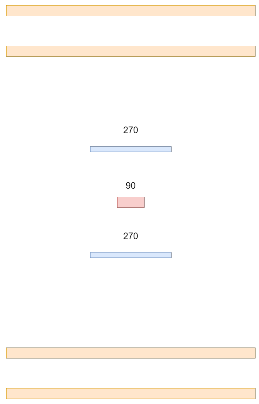

Figure 20: Shielding configuration for Towers 9, 10. Signal line shown in red and shields in blue.

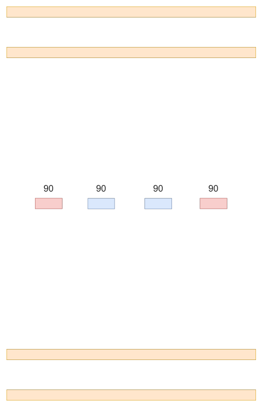

Figure 21: Shielding configuration for Tower 11. Signal line shown in red and shields in blue.

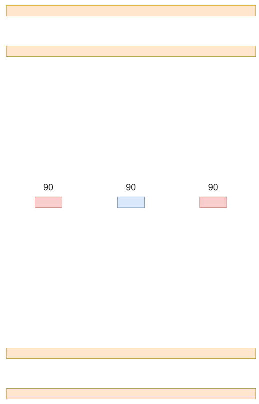

Figure 22: Shielding configuration for Tower 12. Signal line shown in red and shields in blue.

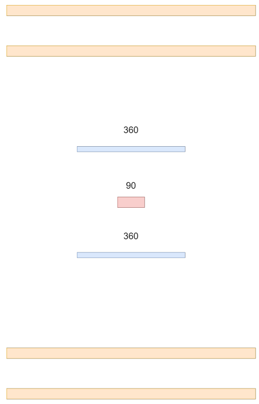

Figure 23: Shielding configuration for Tower 13. Signal line shown in red and shields in blue.

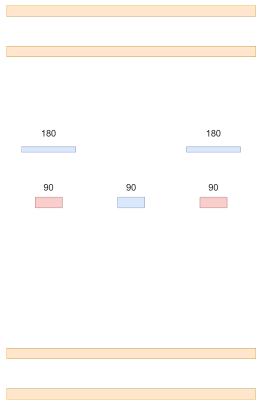

Figure 24: Shielding configuration for Tower 14. Signal line shown in red and shields in blue.